A Radiation-Hardened, High-Resolution Optical Encoder for Use in Aerospace Applications

Pat Kreckie*

Abstract

Advances in aerospace applications have created a demand for the development of higher precision, higher accuracy, radiation-hardened encoders. Historically, encoder products have proved somewhat deficient due to precision, accuracy, weight, and alignment concerns. MicroE Systems' Mercury II aerospace encoder design provides the precision and accuracy required by these applications while also addressing radiation, weight, and alignment concerns. The encoder is a grating-based, reflective, interferometric encoder consisting of three major components: a scale, a readhead, and processing electronics. The system is a kit design that is easily configured and forgiving of misalignments. Its large tolerance of tilts and translations during setup and operation, make this design ideal for aerospace requirements. The system is small in footprint and weight and requires minimal power for operation. The ability to attach multiple readheads to one processing electronics unit, as well as its alignment tolerances, makes it versatile enough to meet the most demanding applications.

Background

An optical encoder is a device that uses optical sensing of some sort to determine the position of a surface with respect to the system's sensor head. Typical systems consist of a scale, a sensor head(s), and processing electronics (Figure 1). Encoder systems may be linear or rotary, reflective or transmissive, kit or packaged, incremental or absolute.

MicroE Systems' Mercury II encoders are grating-based interferometric encoders. Light from a source within the sensor head is incident on the scale. The scale attaches to the surface being monitored. The scale is a glass substrate containing a periodic grating structure. The incident light reflects and diffracts from the grating. The diffracted beam re-enters the sensor head and forms interference fringes on a detector array. The processing electronics calculate the interference fringe pattern's spatial phase from the detector array signals. Scale movement (surface movement) results in fringe pattern movement across the detector array. The processing electronics re-analyze the resulting fringe pattern and produce a system output corresponding to the surface's new position.

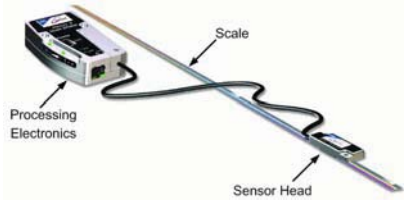

Figure 1. Encoder Components

* MicroE Systems, Natick, MA

Optical Design. The optical system (Figure 2) consists of multiple light sources, a window, a scale, and a detector. Single-mode vertical cavity surface emitting lasers (VCSEL) are the system's light sources. Each VCSEL emits 850nm diverging beams with excellent spatial and spectral coherence. In this design, four VCSELs are used – primary and redundant VCSELs for the Main signals and primary and redundant VCSELs for the Index signals. Although VCSEL lifetimes are excellent, the redundant set further improves the reliability of the system. VCSELs offer many advantages over other laser sources including excellent mode stability, low current draw, and very long lifetime. The vertical cavity design allows for emissions from the surface of the die, simplifying its mounting, eliminating the need for additional beam directing optics and facilitating an extremely small system footprint.

Scale Design – Main Track. The Main and Index VCSELs illuminate the Main Track and Index Track sections of the scale, respectively. Each VCSEL generates a diverging beam that passes through a window (not shown) and exits the sensor head.

The scale's Main Track section is an optical chrome-on-glass grating with a 20-µm period. The incident Main VCSEL beam reflects and diffracts into multiple overlapped beams from this scale region (Figure 3).

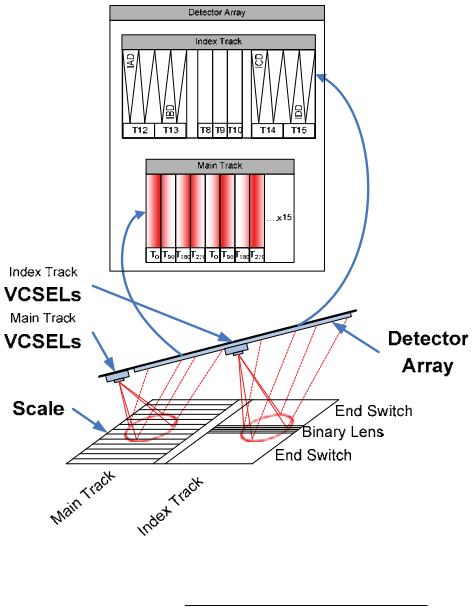

Figure 2. Optical System Layout

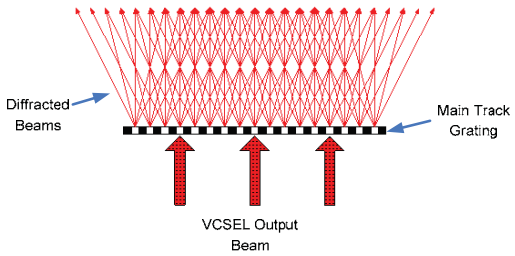

Figure 3. Main Track Diffracted Beams

These beams reenter the sensor and illuminate a four-channel Main Track detector array. Since multiple coherent beams overlap on the detector, interference fringes form on the Main Track array (Figure 2) according to the well-known Talbot effect. This effect, when illuminating with a point source, governs the shape, period and contrast of the fringes. [1]

Due to the grating's square-wave design with a duty cycle of roughly 50-50, the even diffracted orders are suppressed and the fifth and higher orders are relatively weak leaving the zero, first and third orders as dominant. The Gaussian distribution of the VCSEL beam further reduces the power of the higher orders at the detector; so the interference fringes formed at the detector are primarily generated by the interference of orders 0, 1 and 3. The detector is situated in a Talbot plane where the grating is "self imaged"; so, given the limited set of orders contributing to the interference, the fringes consist mainly of the fundamental with the third harmonic.

As the scale moves, the diffracted orders shift either up or down by various amounts depending on the order of each particular diffracted beam. This phase shifting causes the interference fringes to move across the array resulting in a modulated current from the detector. Given fringes that are well defined by the physics of the Talbot effect, the resulting signal modulation is predictable and controllable.

Scale Design – Index Track. The Index Track section of the scale contains three regions: two (2) end switches and a binary lens (Figure 2). The end switches are highly reflective regions used in the continuous automatic gain control of the VCSELs' output energies during operation. The binary lens region is the index mark for the system. The binary lens creates a focused line of light on the detector as the index VCSEL beam sweeps across this region. This index pulse defines the "home" position of the system. Because the binary lens is a physical reference on the scale, it is highly repeatable.

Detector Design – Main Track. The detector is a silicon photodiode with excellent response at the 850 nm wavelength of operation. The die has two separate arrays: one for sensing the main encoder position signals (Main Track) and one for detecting the index pulse (Index Track) (Figure 2). The main detector region is an interleaved array of 120 cells grouped together to generate four output signals T0, T90, T180 and T270. One optical fringe spans four of the cells, with each of those cells feeding one of the four output channels with a spatially phased modulated current.

There are 30 detector quads and 30 fringes across the length of the main array (Figure 2). The detector samples the sinusoidal optical fringe pattern every 90°: 0°, 90°, 180°, 270°. By grouping the photodiodes in an interleaved fashion, each signal is the averaged sum over 30 periods across the entire fringe pattern. These four signals are amplified and differenced to create the analog sine and cosine signals, which are subsequently digitized and interpolated.

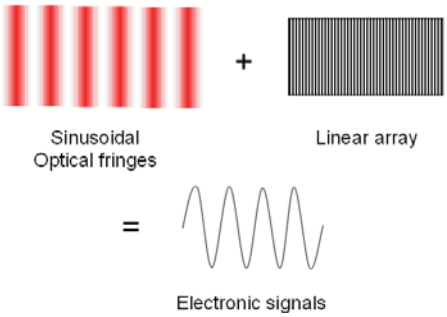

Unlike conventional encoders, small sensor-to-grating gap changes do not have a detrimental or unpredictable impact on the fringe quality. Therefore, the detector and electronics can be designed with foreknowledge of the fringe characteristics, and tuned for the very best response and filtering. In particular, the main detector array cells have been designed to filter out the third harmonic in the interference fringe pattern. These active cells are arranged in a zigzag pattern (Figure 4).

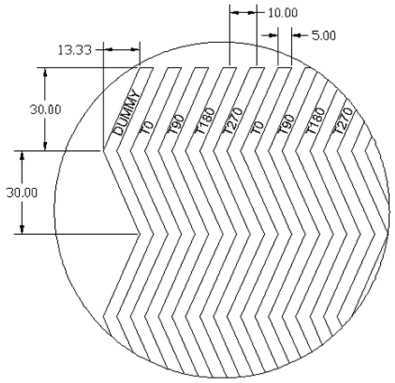

Figure 4. Main track array (dimensions in microns)

The zigzag shape causes the cells to cut across the fringes over a prescribed distance, washing out the third harmonic to generate high fidelity sinusoids, thereby ensuring very high encoder accuracy. With optical harmonic distortion minimized, only electrical offset, electrical gain mismatch, and electrical distortion remain as the primary sources of error.

Detector Design – Index Track. The detector's Index Track is separated into three (3) regions: two (2) end switches and one (1) index region (Figure 2).

As the Index VCSEL beam sweeps across the scale's end switch regions, the beam uniformly reflects onto the Index region of the detector. The detector's end switch regions sample the beam's energy and perform automatic gain adjustments to the detector's signal amplifiers and a current adjustment to the corresponding VCSEL.

As the Index VCSEL beam sweeps across the scale's binary lens, the resultant line of focused light is incident on the detector's index region. The index region consists of 3 cells arranged in a linear array. As the grating moves, the focused line of light sweeps across this three-cell array generating three analog pulses. Comparator circuitry generates a very robust *index window* (IW) digital pulse, roughly one main track cycle wide. The IW is subsequently gated with the interpolator output to yield a one-LSB wide index pulse.

Mechanical Design and Alignment Tolerances. The encoder system accommodates multiple angular and translational motions. Conventional encoders based on geometric optics typically require the alignment between the sensor head and the scale remain within very tight tolerances. In contrast, the interferometric approach employed in the aerospace encoder system permits both a large operating gap between sensor and scale and a very generous operational alignment envelope.

By using a diverging beam from a VCSEL light source, the encoder sensor head can tip and tilt with respect to the scale, while still directing sufficient energy to the grating that diffracts and reflects back to the sensing array in the head. The diffracted beams overlap throughout a large distance along the optical z-axis to form interference fringes that are sensed by the array anywhere within that region. Because the system does not have an intermediate optic between the scale and the detector, the optical fringes do not distort throughout the alignment tolerance range (Figure 5).

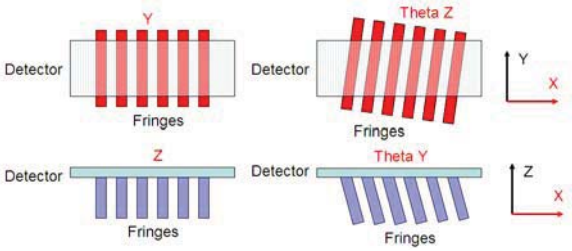

Figure 5. Sensed interference fringes

These key features differentiate the Aerospace Encoder from other options. The very forgiving initial alignment conditions and the large tolerance of tilts and translations along axes other than the measurement axis during encoder operation, make this design ideal for aerospace requirements. Table 1 outlines the alignment tolerances of the Aerospace Encoder. The values reported in the table are based on reduction in analog signal amplitude only and represent a conservative range.

Table 1. Alignment Tolerances

Axis	Mercury II Aerospace
Y	± 300 µm
Z	± 200 µm
Theta Z	± 2°

For ultimate stability through temperature, the sensor mounts with either screws or adhesive along the y-axis in line with the VCSEL and detector, thereby minimizing drifts due to thermal expansion.

Electrical Design. The electronics design is based upon the second generation of MicroE's Mercury incremental encoder. All of the analog signal processing is performed in a mixed mode ASIC, while the digital processing occurs in an FGPA. A/D converters provide the interface between the analog signals and the digital signal processing. The signal processing is ratiometric, making it insensitive to common mode changes, and the processing algorithms utilized are either not affected by single event upsets (SEU) or quickly recover from upsets without permanent change. For more information, see the Upset Effects section.

Analog Signal Processing. All analog signal processing is performed in a mixed mode ASIC. There are 4 signals generated from the multi-element, interleaved, main track photodetector array (0°, 90°, 180°, and 270°). Transimpedance amplifiers convert these currents to voltages. The 0° and 180° signals are subtracted and amplified to form differential, high-level sine signals while the 90° and 270° signals are subtracted and amplified to form differential, high-level cosine signals. The signals from one photodetector section combine with the corresponding signals in the other. The high signal to noise ratio obtainable in the design provides high-speed operation and still interpolates to 14 bits (1.22 nm). This high signal-to-noise ratio also allows for a low noise encoder.

The combined sine and cosine signals are applied to a dual, high speed, A/D converter, located in the sensor head. Three index signals generated from the detector array form the index window used to identify a home position. The Transimpedance amplifiers convert the index currents to voltages in the ASIC. These signals are processed to form two complementary, high-level signals, which, in turn are applied to the inputs of a comparator. The comparator output is the index window. Additional processing occurs during the digital signal processing.

The ASIC also contains the laser drivers. These are controllable current sources, with built-in over-current protection for the VCSELs and circuitry for selecting either the primary or the redundant VCSELs.

Digital Signal Processing—All digital signal processing is performed in the FPGA. The serial outputs from the two A/D converters in each sensor head are applied to the FPGA through RS-422 receivers. This FPGA applies gain, offset, and phase correction, interpolates the signals from each of the sensor heads to 14 bits (1.22 nm), counts fringes, defines the home position from the index window, formats the output signals and provides timing signals.

Cyclic Error—For gain, offset, and phase (GOP) correction, the system uses a patented GOP correction algorithm that iteratively reduces gain, offset, and phase errors by sensing the respective GOP errors and adding correction coefficients to the sine and cosine signals.

Once the correction factors are fully reduced, they are fixed so that the encoder position is repeatable, as shown in Figure 6 and Figure 7.

The Lissajous is a graphical depiction of sine versus cosine. Lissajous roundness is used to measure cyclic error along with encoder position verses reference. Note that a change in the vector length of the Lissajous does not result in a position change.

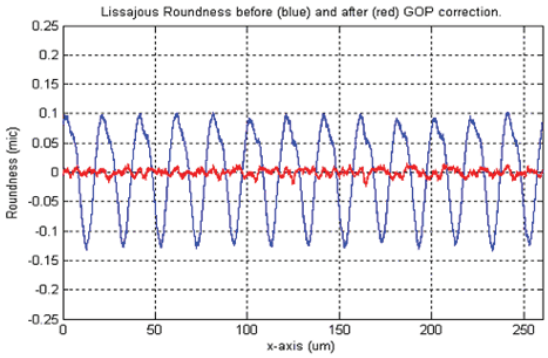

Figure 6. Typical MII Lissajous roundness cyclic error correction

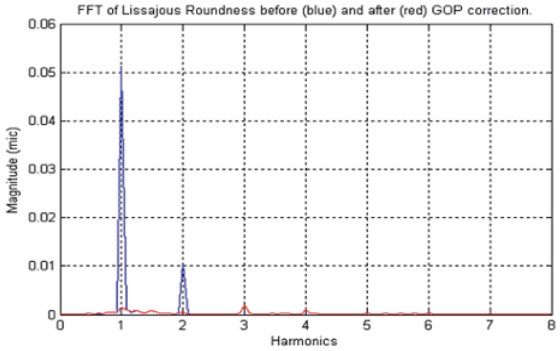

Figure 7. Typical MII Lissajous FTT cyclic error correction

A/D conversion and interpolation—To ensure proper fringe counting, the A/D conversion and interpolation rate is considerably high. The highly effective calibration/correction algorithm developed by MicroE provides extremely high accuracy (see the Accuracy Section below).

To take advantage of the algorithm at any time, enable the Calibration mode and pass over 40 fringes. The digital processing also provides an accessible troubleshooting mode. Parameters such as signal amplitude, laser current, and signal speed are exportable.

To maintain a constant input signal level to the A/D converters, an automatic gain control (AGC) loop varies the VCSEL current. This loop uses the vector magnitude of the main track as the control. If the required magnitude cannot be obtained (to within a predetermined percent of the target amplitude), the circuit will switch to the redundant VCSEL.

Operation of the index circuitry allows measurement of the index VCSEL power at all times except at the index. This measurement determines whether to select the back-up VCSEL. Due to the large operating signal range of the index circuitry, it is not necessary to use AGC. The fringe counting and index circuitry are robust (see the Fringe Counting section below).

Formatting the output signals is performed within the FPGA. A low voltage differential signal (LVDS) driver/receiver translates the input and output signals from the device. Internal timing synchronizes to a 68 MHz oscillator.

Upset Effects. As previously mentioned, the circuitry and algorithms in the design are either not effected by upsets or quickly recover from upsets with no permanent change. All digital circuitry uses integrated circuits fabricated using radiation-hard processing and all critical registers use triple redundant voting logic to eliminating SEU concerns. Thus, it is only necessary to consider the following three effects on the analog signals: fringe interpolation, fringe counting, and index homing.

Fringe Interpolation. MicroE utilizes an interpolation method that is absolute in nature. It is essentially an arctan method of interpolation. Therefore, if the sine or cosine signal is disturbed, the interpolated value will become incorrect (as it will for any encoder, incremental or absolute), but will recover with the correct position word by the next interrogation as long as the encoder has not moved beyond one optical fringe; i.e., one analog signal cycle.

Fringe Counting. The algorithm utilized for fringe counting only allows the count to change when the sine transitions from the fourth to first quadrant (increase count) or the first to fourth quadrant (decrease count) and ignores the all other quadrant changes. In order to miss a count, the disturbance would have to be larger than the peak amplitude of the normal signal, effectively eliminating one of the quadrants. Radiation analysis indicates that the amplitude of the upset signals is more than an order of magnitude lower than this.

Index Homing. The index circuit uses the index window to determine which fringe is *home*. The algorithm that determines this *home* position requires that the index window be a minimum of one-half fringe wide. Under normal rate conditions, this is a minimum of 100 µs. Since any upset signal will decay with a time constant of 1.7 µs (due to the system bandwidth), it is not possible for an upset to be present for 100 µs.

Accuracy. The Aerospace sensor has several improvements over older encoder models. In particular, the detector is larger for better averaging and robustness and the array pattern modified for better signal filtering as mentioned earlier; these all contribute to enhance intrafringe accuracy.

Note the Aerospace Encoder's enhanced harmonic suppression and the low error of 18-nm peak—a dramatic reduction of approximately 4x down from the typical 70 – 80 nm peak error of previous models. In addition to these short-range accuracy improvements, the Aerospace Encoder's long-range (interfringe) accuracy improved due to the larger sampling area and a shorter optical path length between the grating and the sensor head.

Radiation—MicroE uses radiation-hardened integrated circuits for the encoder electronics. Due to the inherent radiation hardness of GaAs, radiation environments do not present a problem for the VCSELs in the encoder. Data shows that the primary effect of high dose radiation on VCSELs is a moderate reduction in output power. The encoder design accommodates these levels of changes. The VCSEL driver design utilizes AGC to maintain a constant output power further mitigating the effects of radiation.

Conclusions

The Mercury II Aerospace Encoder provides many advantages over standard encoders:

- Small, low-mass sensor with ultra low Z-height fits in compact motion systems
- Superior resolution and accuracy - resolutions up to 1.22nm (linear), 268M CPR (rotary); interpolation accuracy of ≤ 30 nm mean, std. dev. 4 nm (linear glass scales); up to ± 1 µm (linear glass scales up to 130-mm long)
- High-speed operation - up to 2.5m/s at 0.1-µm resolution
- Versatility - one sensor works, linear or rotary glass scales
- Broad sensor alignment tolerances, built-in red/yellow/green setup LEDs, and pushbutton setup make sensor, index and limit setup fast and eliminate ancillary setup instruments
- Large alignment tolerances
- Large range of thermal performance
- Proven solid history as reliable and dependable
- Robustness features include all differential digital outputs, all digital signals from the sensor, and double-shielded cabling for superior EMI/RFI immunity; scale contamination resistance insures encoder operation even with fingerprints, oil, dust and other forms of contamination

References

[1] Emil Wolf, Editor, Progress in Optics, Volume XXVII North Holland, Publisher, 1989